Am J Transl Res 2020;12(9):5586-5596
www.ajtr.org /ISSN:1943-8141/AJTR0109696

Original Article

Simvastatin ameliorates oxygen glucose deprivation/reoxygenation-induced pulmonary endothelial barrier dysfunction by restoring cell-cell junctions and actin cytoskeleton dynamics via the PI3K/Akt signaling pathway

Dong Han[1*], Junjun Sun[1], Dikun Fan[1], Chao Zhang[1], Shoufeng Du[1], Wang Zhang[2*]

[1]*Department of Cardiovascular Surgery, The Central Hospital of Nanyang, Nanyang, Henan, PR China;*
[2]*Department of Critical Care Medicine, The First Affiliated Hospital, College of Medicine, Zhejiang University, Hangzhou, Zhejiang, PR China.* [*]*Equal contributors.*

Received February 22, 2020; Accepted August 1, 2020; Epub September 15, 2020; Published September 30, 2020

Abstract: Endothelial barrier dysfunction is a critical pathophysiological process of pulmonary ischemia/reperfusion (I/R) injury in patients scheduled for cardiopulmonary bypass. Impaired actin cytoskeleton dynamics and cell-cell junctions are the main causes of endothelial dysfunction. Statins have protective effects on I/R-induced lung injury; however, the mechanism is unclear. We explored the therapeutic potential of simvastatin (SV) in endothelial cells subjected to oxygen-glucose deprivation/reoxygenation (OGD/R). SV pretreatment promoted the barrier function of human pulmonary microvascular endothelial cells (HPMECs) subjected to OGD/R. LY294002 was used to evaluate the role of the PI3K/Akt pathway in regulating the barrier function of HPMECs subjected to OGD/R. LY294002 suppressed the barrier function of HPMECs. SV restored the endothelial barrier function by rescuing endothelial cell migration and permeability, which are involved in the regulation of cytoskeleton dynamics and intercellular junction expression via the PI3K/Akt signaling pathway.

Keywords: Simvastatin, oxygen glucose deprivation, endothelial injury, cell junction, cytoskeleton

Introduction

Lung ischemia-reperfusion injury (LIRI), a type of lung injury caused by aseptic inflammation, is common in lung transplantation, extracorporeal circulation, trauma, pulmonary embolism, and surgery [1-3]. Activation of immune system (such as neutrophils and platelets, cytokines, and the complement system) caused by oxygen-glucose deprivation/reoxygenation (OGD/R) is thought to be related to LIRI [4]. The resulting pulmonary vascular endothelial cell injury and related endothelial barrier dysfunction is a key pathophysiological process of LIRI [1]. Cytoskeletal rearrangements related to cell migration and disruption of cell-cell junctions are major causes of increased vascular permeability [5, 6].

Statins inhibit HMG-CoA reductase [7]. In addition to their lipid-lowering effects in coronary artery disease, statins have anti-inflammatory effects, induce nitric oxide synthase (NOS), and affect leukocyte adhesion and translocation [8-10]. They are thus implicated in inflammatory diseases such as autoimmune disorders, multiple sclerosis, chronic obstructive pulmonary disease, acute respiratory distress syndrome (ARDS), and sepsis [11-13]. Statins protect against ischemia-reperfusion injury in the myocardium [14], lung [15], and liver [16], and clinical studies have confirmed the protective effects of simvastatin (SV) in the lung [17-19].

The PI3K/Akt signaling pathway is the main regulator of endothelial barrier function during LIRI [20, 21], and regulates endothelial cell migration via cytoskeletal rearrangement [22]. Several drugs, such as dexmedetomidine and sevoflurane, protect against LIRI by activating the PI3K/Akt pathway, a key therapeutic target [21, 23]. Here we investigated whether SV pro-

tects the vascular endothelium and repairs OGD/R-injured endothelial cells via the PI3K/Akt signaling pathway.

Material and methods

Cell culture

HPMECs (Cat. No. 3000; ScienCell, San Diego, CA, USA) was cultured in Endothelial Cell Medium (ECM, Cat. No. 1001; ScienCell) supplemented with 5% (v/v) Fetal Bovine Serum (FBS, Cat. No. 0025; ScienCell), 1% endothelial cell-derived growth factor (ECGS, Cat. No. 1052; ScienCell), and 1% penicillin-streptomycin (Cat. No. 0503; ScienCell). Cells were incubated at 37°C and 5% CO_2. SV (Cat. No: S6196, Sigma, Germany) was added to HPMECs for pretreatment at a concentration of 1 μmol/L. PI3K inhibitor LY294002 (Cat. No: S1105, Selleck, USA) were diluted with ECM without FBS and used at a concentration of 25 μmol/L. To mimic lung I/R in vitro, OGD/R was performed as described previously [24], briefly, HPMECs were washed twice with phosphate-buffered saline (PBS, pH 7.4) and then incubated in a hypoxia chamber (containing a gas mixture of 5% CO_2 and 95% N_2) at 37°C to produce OGD condition, After 4 h of anaerobic culture, cells were then incubated in complete ECM for 24 h at 37°C and 5% CO_2.

Transwell-Evans blue monolayer permeability assay

HPMECs were seeded (1 × 10^5 cells per well) on a Transwell plates (#3472, pore size: 3.0 μm, CoStar; Corning Inc.), then grown for 5 d with complete ECM, After the cells exposed to OGD/R, the ECM in the insert was replaced with 100 μl EvansBlue (EB, Cat. No. E2129; Sigma)-conjugated albumin (4% BSA, final concentration of EB-BSA: 0.67 mg/ml) as previously described [25]. The medium in the lower chamber was replaced with the 500 μl BSA (4%). After incubating for 1 h at 37°C in 5% CO_2, the sample in the lower chamber was collected and determined at 620 nm using a micro-plate reader.

Trans-endothelial electric resistance measurements

Endothelial monolayer barrier function was measured by trans-endothelial electrical resistance (TEER) using an electrical resistance system (Millicell-ERS, MERS00002; Merck Millipore, Germany). HPMECs were seeded (1 × 10^6 cells per well) on a Transwell plates (#3470, pore size: 0.4 μm, CoStar), then grown for 5 d with complete ECM, After the cells exposed to OGD, electrical resistance across the monolayer was measured in Ohms (Ω) and TEER was calculated based on the manufacturer's recommendations.

Cell viability assay

The cell viability of HPMECs was assessed by Cell Counting Kit-8 (CCK-8; Dojindo, Tokyo, Japan) assay as described previously [26]. Cells were seeded on 96-well plates at the concentration of 10^4/ml. After OGD/R and SV treatments, cells were incubated with CCK-8 solution for 2 h at 37°C, the absorbance was determined at 450 nm using a micro-plate reader.

Wound healing assay

Cell migration was determined through a wound healing assay as described previously [26], briefly, when HPMECs became confluent in 6-well plates, a wound was scraped by using a 200 μl pipette tip and then washed with PBS to remove the cell debris. Images of the wound were acquired by using the microscope. After further incubated for 24 h in ECM with 1% FBS, the wound images were acquired again. The migration ability was measured by the rates of scratch wound confluence using Adobe Photoshop 2017 software (Adobe Systems Inc, San Jose, CA, USA).

Transwell migration assay

HPMECs were seeded (2 × 10^4 cells per well) in 100 μl of serum-free ECM on a Transwell plates (#3464, pore size: 8.0 μm, CoStar), after OGD/R and SV treatments, cells with Transwell inserts were washed with PBS and then fixed in 4% (w/v) paraformaldehyde solution for 20 min. Non-migrating cells on the surface of the insert were removed by using a cotton swab and then washed three times with PBS. Next, the inserts were stained with crystal violet for 10 min and washed three times with PBS. The inserts membrane was observed under a microscope and cell number was counted from three random fields.

Immunofluorescence staining

HPMECs were treated as we described previously [27], briefly, the cells were fixed in 4% (w/v) paraformaldehyde solution, washed with PBS and incubated with anti VE-Cadherin Rabbit antibody (1:400, #2500; Cell Signal Technology, USA) and Claudin-5 Rabbit antibody (1:200, Cat. No. ab15106; Abcam, Cambridge, MA, USA) overnight at 4°C. After washing with PBST, cell was incubated with FITC-phalloidin (Cat. No: P5282; Sigma, Germany) or secondary antibody (CoraLite594-conjugated Goat Anti-Rabbit IgG(H+L), 1:200, Cat. No. SA00013-4; CoraLite594-conjugated Goat Anti-Rabbit IgG(H+L), 1:200, Cat. No. SA00013-4; Proteintech), then washed with PBST and incubated with DAPI (1:2000, Cat.No. D9564; Sigma-Aldrich). Fluorescent pictures were captured with the FV-1000 confocal microscope (Olympus, Tokyo, Japan).

Quantitative real-time PCR (qRT-PCR)

For gene expression assay, total RNA for each cell group was extracted and reverse-transcribed to cDNA in accordance with the manufacturer's instructions (Cat. No. RR036A; TaKaRa, Tokyo, Japan). RT-PCR reaction with the 7500 RT-PCR (Applied Biosystems, Life technologies, Carlsbad, CA) was performed at 95°C (30 s) followed by 40 cycles at 95°C (5 s)/60°C (30 s), SYBR greenintercalating dye (Cat. No. RR820L; TaKaRa) was used for signal detection. Primers for these reactions: VE-Cadherin, 5'-CGAGAGCTACACGTTCACGG-3' (forward), 5'-GGGTGTCGAGGGAAAAATAGG-3' (reverse); Claudin-5, 5'-CTCTGCTGGTTCGCCAACAT-3' (forward), 5'-CAGCTCGTACTTCTGCGACA-3' (reverse); GAPDH, 5'-GGAGCGAGATCCCTCCAAAAT-3' (forward), 5'-GGCTGTTGTCATACTTCTCATGG-3' (reverse).

Western blot

Total proteins of HPMECs were extracted as described previously [27], protein sample were separated in SDS-PAGE and transferred to the polyvinylidene difluoride (PVDF) membrane (Cat. No. IPVH00010; Merck Millipore, Germany). The membranes were incubated for 1 h in 5% (w/v) skim milk-Tris-buffered saline supplemented with 0.1% (v/v) Tween-20 (TBST). Membranes were then incubated at 4°C overnight with primary antibodies including VE-Cadherin (1:1000, #2500; Cell Signaling Technology), Claudin-5 (1:1000, ab15106; Abcam, Cambridge, MA, USA), Akt (1:1000, #4685, Cell Signal Technology, USA), p-Akt (1:2000, #4060, Cell Signal Technology, USA) and GAPDH (1:1000, #5174, Cell Signal Technology, USA). The membranes were then washed three times with TBST, then incubated for 1 h at room temperature with HRP-conjugated anti-rabbit antibody (1:5000, #7074; Cell Signaling Technology). The membranes were developed with enhanced chemiluminescence kit (Cat. No. 70-P1421; MultiSciences Biotech, Hangzhou, China).

Statistical analysis

All data were expressed as mean ± standard deviation (SD). Two-tailed Student's t-tests was used for two-group comparisons, one-way analysis of variance (ANOVA) was used for multiple-groups comparisons, Tukey's multiple comparisons test was used after one-way ANOVA. GraphPad Prism 7.0 (GraphPad Software Inc., San Diego, CA, USA) was used for analysis. The difference was statistically significant at $P < 0.05$.

Results

SV reduces the high monolayer permeability and increases the low trans-endothelial electric resistance (TEER) of HPMECs induced by OGD/R

We investigated the effects of SV on the endothelial barrier function of HPMECs after OGD/R by assaying monolayer permeability and TEER. As expected, OGD/R significantly decreased TEER, which indicates decreased barrier integrity. However, TEER was significantly higher in the SV-pretreated group than in the OGD/R group (**Figure 1A**). Similar results were found in Transwell-Evans Blue (EB) leakage assays. The leakage of EB from the Transwell inserts, reflecting monolayer permeability, was increased in the OGD/R group compared to the control group, and in the SV group compared to the OGD/R group (**Figure 1B**). CCK-8 assays showed that cell viability was significantly decreased by OGD/R and OGD/R+SV, although there were no significant differences in cell viability between the OGD/R and OGD/R+SV groups (**Figure 1C**). Therefore, the effects of SV on OGD/R-induced pulmonary endothelial bar-

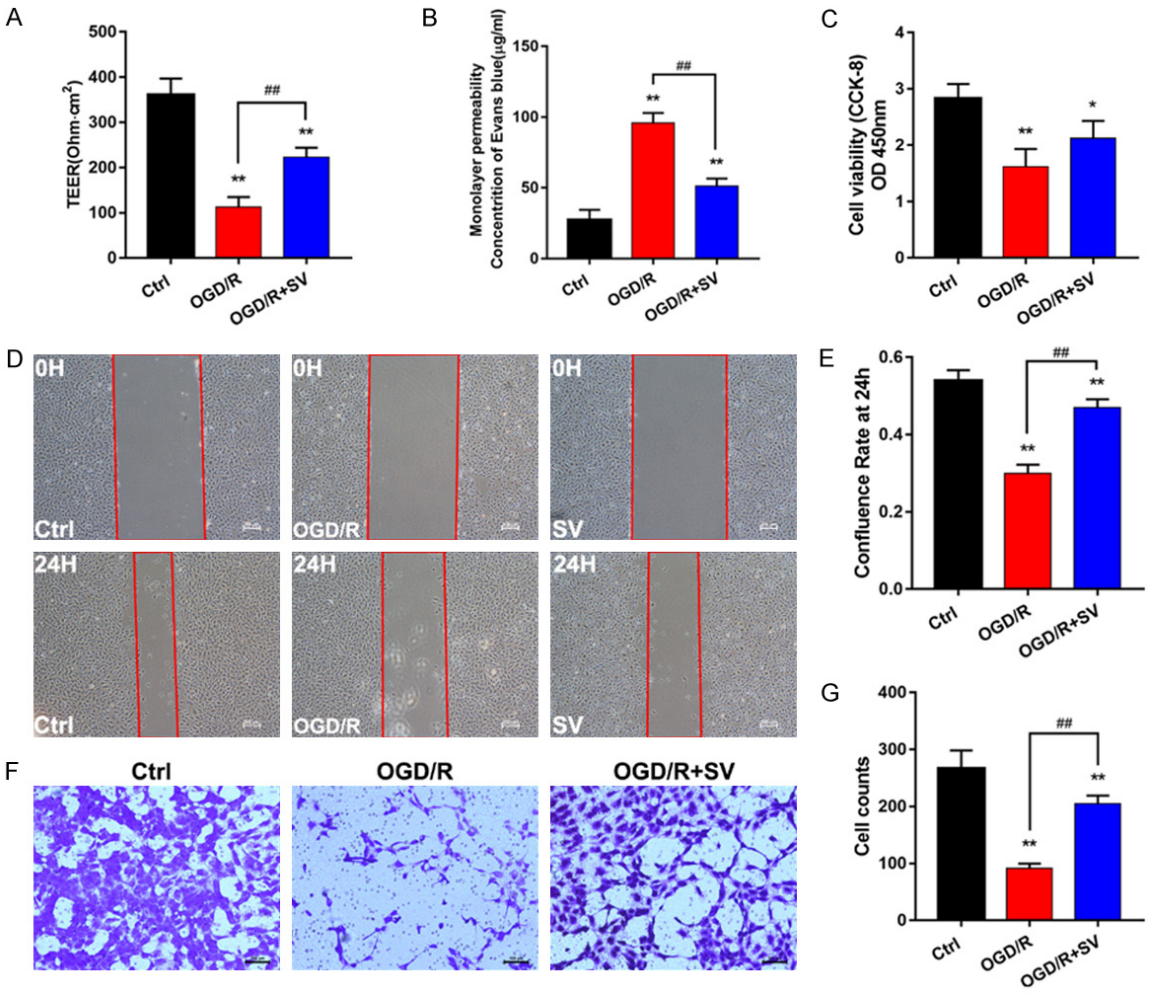

Figure 1. Effects of SV on TEER, monolayer permeability, and migration of OGD/R-treated HPMECs. A. The TEER of HPMEC monolayers decreased in the OGD/R group and was higher in the SV group (all Ps < 0.01). B. Leakage of EB was increased in the OGD/R group compared to the control and SV groups (all Ps < 0.01). C. Cell viability was significantly lower in the OGD/R group than in the control group (P < 0.01). There were no significant differences between the OGD/R and SV groups. D, E. Quantification of confluence at 24 h as an indicator of migration ability (% wound confluence = [a-b] × 100%/a; a = initial scratch wound area at 0 h, b = scratch wound area at 24 h). E. Migration of HPMECs subjected to OGD/R was decreased in the control and SV groups (all Ps < 0.01). Scale bars, 200 μm. F, G. The number of migrated cells was significantly lower in the OGD/R group than in the control and SV groups (all Ps < 0.01). Scale bars, 100 μm. Data are from three independent experiments, error bars represent standard deviations. *P < 0.05 vs. control group, **P < 0.01 vs. control group, ##P < 0.01.

rier dysfunction may not be mediated by modulation of cell viability.

SV remodels the cytoskeleton and increases migration after OGD/R

To determine the effects of SV on HPMEC migration after treatment with OGD/R, we measured migration rates using a wound-healing assay. The extent of scratch wound confluence at 24 h was significantly less in the OGD/R group than in the control and SV-pretreated groups (**Figure 1D** and **1E**). Cell migration was measured with a Transwell migration assay. The number of migrated cells was significantly lower in the OGD/R group than in the control group. However, SV pretreatment increased the number of migrated cells (**Figure 1F** and **1G**). Actin fibers were stained with fluorescein isothiocyanate (FITC)-phalloidin. The actin fibers in HPMECs were visible and regularly arranged beneath the cell membrane in the control group. Cytoskeletal remodeling (disorderly arrangement, different thicknesses, unevenly dis-

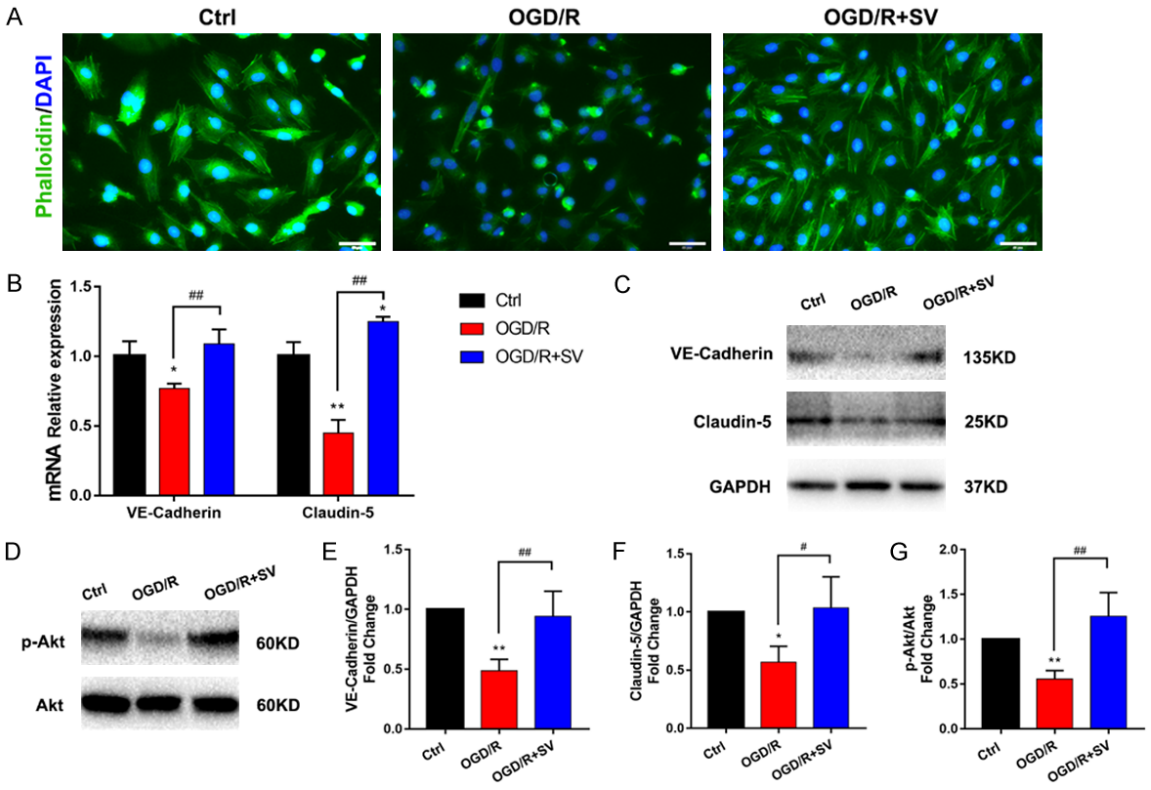

Figure 2. Effects of SV on the cytoskeleton, AJ/TJ expression, and Akt phosphorylation in OGD/R-treated HPMECs. A. FITC-phalloidin staining showed cytoskeletal changes in HPMECs subjected to OGD/R in the presence or absence of SV. Green, phalloidin; blue, nuclei. Scale bar, 50 μm. B. mRNA levels of VE-cadherin and claudin-5 were decreased by OGD/R ($P < 0.05$ and $P < 0.01$, respectively) and were higher in the SV group than the OGD/R group (all Ps < 0.01). C, E, F. Western blotting showed that the protein level of VE-cadherin and claudin-5 were decreased by OGD/R ($P < 0.05$ and $P < 0.01$, respectively) and increased in the SV group compared to the OGD/R group ($P < 0.05$ and $P < 0.01$, respectively). D, G. The ratio of p-Akt to total Akt protein was increased in the SV group compared to the OGD/R group ($P < 0.01$). *$P < 0.05$ vs. control group, **$P < 0.01$ vs. control group, $^{\#}P < 0.05$, $^{\#\#}P < 0.01$.

tributed microfilaments, and a missing cytoskeleton) was observed in the OGD/R group. SV pretreatment partly restored the cytoskeletal structure (**Figure 2A**).

SV increases VE-cadherin and claudin-5 in HPMECs after OGD/R

To ascertain whether SV affects endothelial barrier function by regulating cell-cell junctions, we determined mRNA and protein levels of VE-cadherin and claudin-5. qPCR demonstrated that OGD/R decreased mRNA levels of VE-cadherin and claudin-5. By contrast, pretreatment with SV significantly increased mRNA levels of VE-cadherin and claudin-5 compared to the OGD/R group (**Figure 2B**). Western blotting showed that VE-cadherin and claudin-5 were decreased in the OGD/R group compared to the control group, SV pretreatment resulted in higher protein levels of VE-cadherin and claudin-5 than in the OGD/R group (**Figure 2C**, **2E**, **2F**). Immunofluorescence staining indicated decreased protein levels of VE-cadherin and claudin-5 in the OGD/R group, which were partly recovered in the SV group (**Figure 3A** and **3B**).

SV protects the barrier function of HPMECs against OGD/R-induced injury via the PI3K/Akt pathway

To clarify whether the PI3K/Akt pathway is involved in the effects of SV on endothelial barrier function after OGD/R treatment, we investigated PI3K/Akt pathway activity. Western blotting demonstrated that OGD/R treatment significantly down-regulated the ratio of phosphorylated Akt (p-Akt) to total Akt compared to the control group. SV pretreatment increased the ratio of p-Akt to total Akt in HPMECs after OGD/R treatment (**Figure 2D** and **2G**).

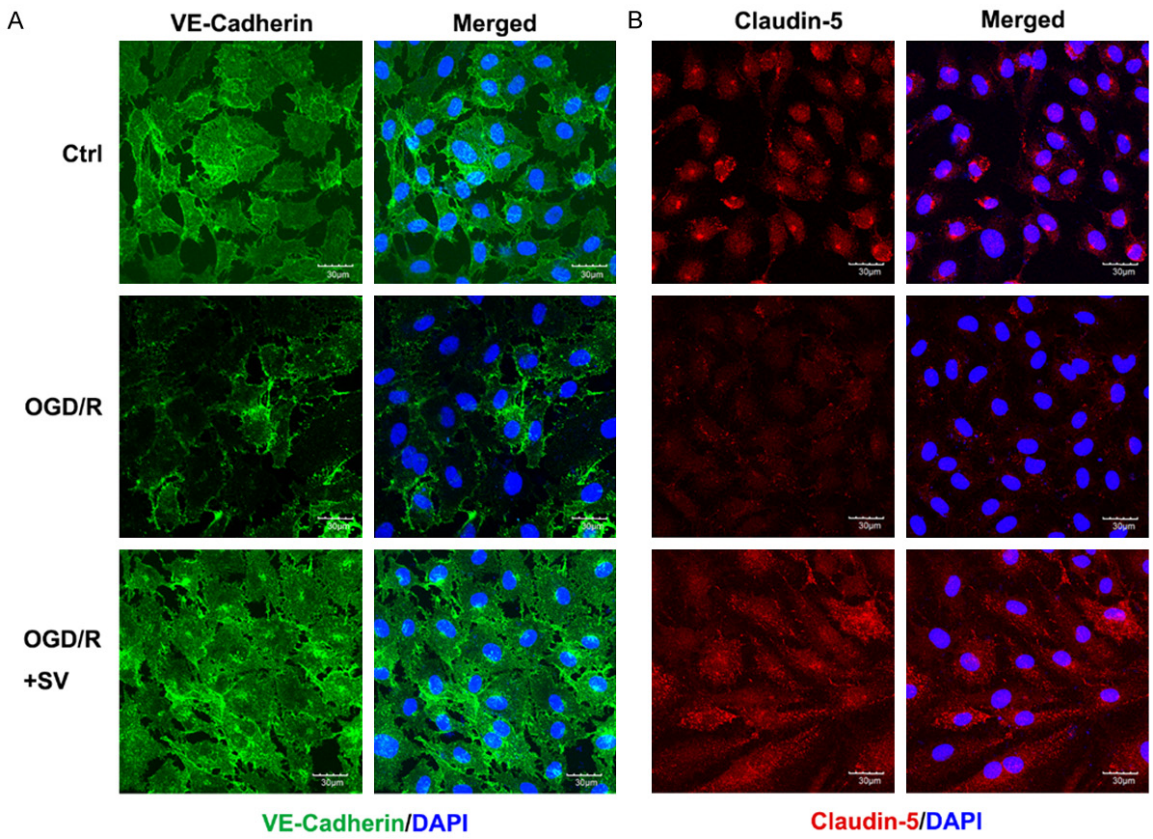

Figure 3. Immunofluorescence staining of VE-cadherin and claudin-5 in OGD/R- and OGD/R+SV-treated HPMECs. A. VE-cadherin expression after OGD/R treatment in the presence or absence of SV. Green, VE-cadherin; blue, nuclei. B. Claudin-5 expression after treatment with OGD/R in the presence or absence of SV. Red, claudin-5; blue, nuclei. Scale bar, 30 μm.

To test whether the protective effects of SV could be reversed by PI3K/Akt inhibition, based on our previous report [27], we used LY294002 (25 μmol/L), a PI3K inhibitor. LY294002 (25 μmol/L) did not significantly affect untreated HPMECs in terms of TEER, monolayer permeability, migration, or Akt phosphorylation (Figure S1). TEER was significantly decreased in the SV+LY294002 group compared to the SV group (**Figure 4A**). Similarly, EB leakage from the upper chamber was increased in the SV+LY294002 group compared to the SV group (**Figure 4B**). The scratch wound confluence rate and the number of migrated cells were significantly decreased in the SV+LY294002 group compared to the SV group (**Figure 4C-F**). In addition, FITC-phalloidin staining showed that actin fibers were tight and ordered in the SV group, but LY294002 significantly reduced the number of actin fibers, which were also thinner, shorter, and more disordered (**Figure 4G**). Therefore, activation of the PI3K/Akt pathway is involved in cytoskeletal remodeling and cell migration.

Finally, we measured adherens/tight junction proteins involved in the PI3K/Akt pathway. qPCR analyses revealed that SV+LY294002 decreased mRNA levels of VE-cadherin and claudin-5 compared to the SV group (**Figure 6A**). Immunofluorescence staining showed that VE-cadherin and claudin-5 were downregulated by LY294002 compared to the SV group (**Figure 5A** and **5B**). Western blotting showed that protein levels of VE-cadherin and claudin-5 in the SV+LY294002 group were significantly lower than those in the SV group (**Figure 6B-D**). The p-Akt level was also reduced by LY294002 (**Figure 6B** and **6E**).

Discussion

Pulmonary I/R is a frequent event that induces distant organ dysfunction and acute lung injury (ALI)/ARDS. These are important compo-

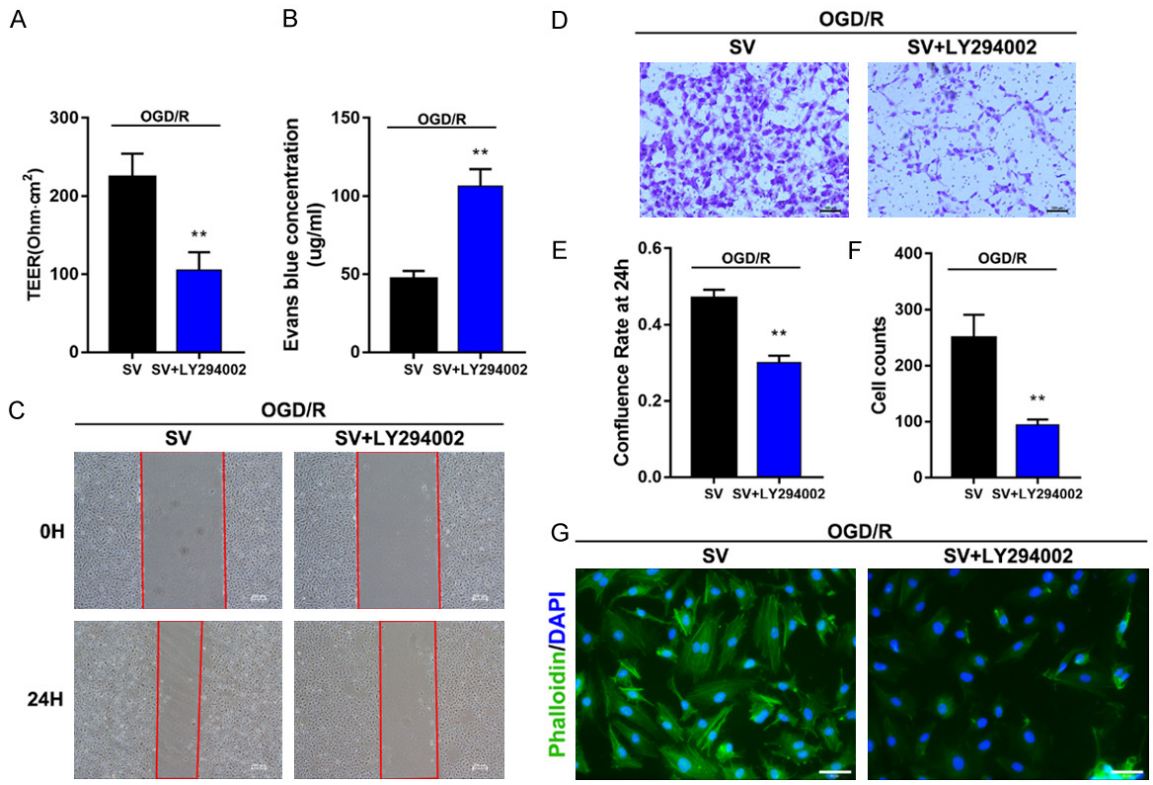

Figure 4. Effects of PI3K/Akt inhibition on TEER, monolayer permeability, cell migration, and the cytoskeleton of OGD/R-injured HPMECs treated with SV. A. The TEER of monolayer HPMECs was decreased in the SV+LY294002 (25 μmol/L) group ($P < 0.01$). B. Leakage of EB was increased in the SV+LY294002 group compared to the SV group ($P < 0.01$). C, E. The migration rate of HPMECs was lower in the SV+LY294002 group than in the SV group ($P < 0.01$). Scale bars, 200 μm. D, F. The number of migrated cells was smaller in the SV+LY294002 group than in the SV group ($P < 0.01$). Scale bars, 100 μm. G. FITC-phalloidin staining showed cytoskeletal changes in HPMECs treated with OGD/R+SV in the presence or absence of LY294002. Green, phalloidin; blue, nuclei. Scale bar, 50 μm. LY294002 (25 μmol/L) had no significant effects on TEER, monolayer permeability, or migration of untreated HPMECs (Figure S1). Data are from three independent experiments, and error bars represent standard deviations. **$P < 0.01$ vs. SV group.

nents of multiple organ dysfunction syndrome [1-3]. Mechanical ventilation is one of the few treatments that reduces the mortality rate of ALI/ARDS; no pathophysiological evidence supports drug treatment [28]. OGD/R-induced inflammation and the associated pulmonary epithelial and endothelial injury are the core events in LIRI and can lead to destruction of the pulmonary barrier, which increases its permeability [1, 4]. The most promising therapies for LIRI focus on reducing pulmonary inflammation and edema and promoting the repair of alveolar epithelial cells and pulmonary vascular endothelial cells [28]. A meta-analysis showed that statins improve the integrity of the cerebral vascular barrier and reduce cerebral edema in animal models of cerebral ischemia [29]. In addition, SV protects the lung by enhancing endothelial barrier function [30]. Therefore, SV has potential as a lung-protective compound. Indeed, in this study the barrier disruption induced by OGD/R was significantly reversed by SV.

Augmentation of cell migration and the strengthening of cell-cell junctions play important roles in the recovery of barrier function. In this study, cell migration was decreased by OGD/R treatment, and this was reversed by SV pretreatment. Dynamic remodeling of the actin cytoskeleton involves a series of important cellular activities, including migration [31]. We found cytoskeletal remodeling in HPMECs after OGD/R injury, but the cytoskeletal structure was partially restored by SV pretreatment, which suggests a role in the barrier function of HPMECs.

Damage to and repair of barrier function likely require dynamic changes in cell-cell junctions.

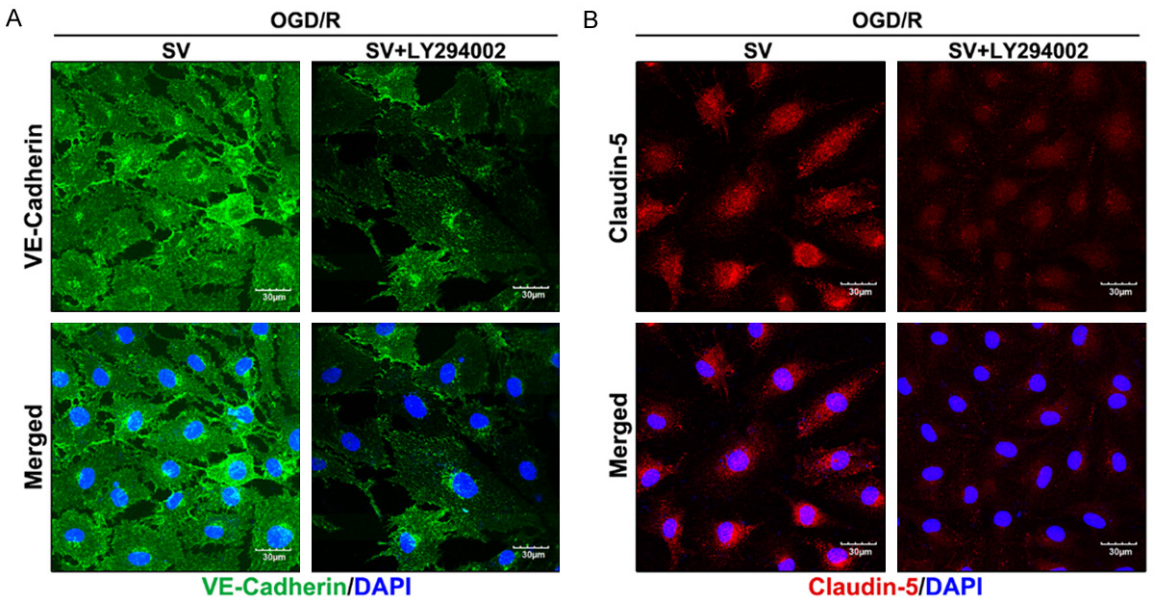

Figure 5. Effects of PI3K/Akt inhibition on VE-cadherin and claudin-5 expression in OGD/R-injured HPMECs treated with SV. A. VE-cadherin expression after OGD/R+SV treatment in the presence or absence of LY294002 (25 μmol/L). Green, VE-cadherin; blue, nuclei. B. Claudin-5 expression after treatment with OGD/R+SV in the presence or absence of LY294002 (25 μmol/L). Red, claudin-5; blue, nuclei. Scale bar, 30 μm.

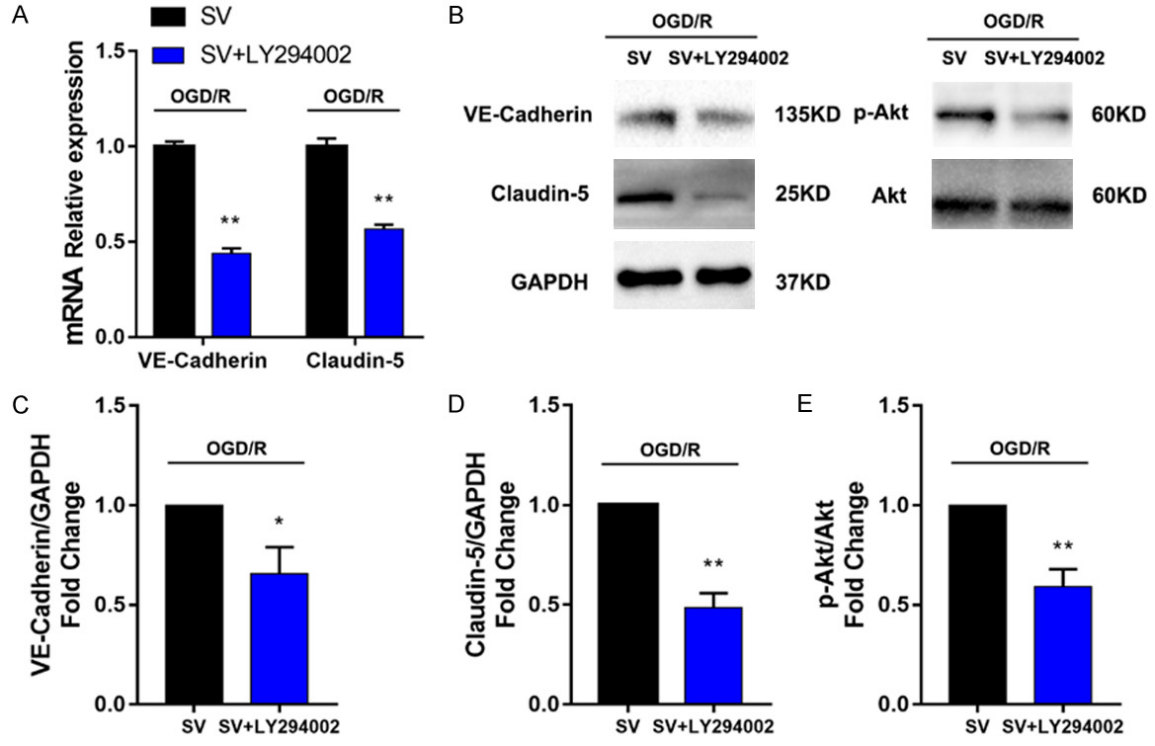

Figure 6. Effects of PI3K/Akt inhibition on VE-cadherin and claudin-5 expression and Akt phosphorylation in OGD/R-injured HPMECs treated with SV. A. mRNA levels of VE-cadherin and claudin-5 were decreased in the SV+LY294002 (25 μmol/L) group compared to the SV group ($P < 0.01$). B-D. Western blotting showed that protein levels of VE-cadherin and claudin-5 were significantly decreased in the SV+LY294002 group compared to the SV group ($P < 0.05$ and $P < 0.01$, respectively). B, E. The ratio of p-Akt to total Akt was decreased in the SV+LY294002 group ($P < 0.01$). LY294002 (25 μmol/L) had no significant effects on Akt activity in untreated HPMECs (Figure S1). *$P < 0.05$ vs. SV group, **$P < 0.01$ vs. SV group.

Adherens junctions (AJs) and tight junctions (TJs) are cell-cell junctions. AJ factors such as VE-cadherin and TJ factors such as claudin-5 are closely associated with barrier permeability in endothelial cells [5, 32]. Downregulation of VE-cadherin causes vascular leakage in patients with ARDS [33]. In addition, Poly (I:C) induces human pulmonary endothelial barrier dysfunction by decreasing expression of claudin-5 in a dose- and time-dependent manner [34]. Similarly, in this study VE-cadherin and claudin-5 expression was downregulated after OGD/R injury and was significantly restored by SV pretreatment.

Our findings demonstrate the importance of actin cytoskeleton remodeling and dynamic changes in cell-cell junctions. However, the way in which cellular signals regulate this process to control barrier function needs to be investigated. The PI3K/Akt pathway is the main regulator of endothelial barrier function during LIRI [20, 21], PI3K/Akt phosphorylation regulates cytoskeletal remodeling, which is crucial for endothelial cell migration [22], as well as expression of cell-cell junctions [35, 36]. We speculate that SV protects the lung by regulating PI3K activity, because Akt activity was upregulated in HPMECs pretreated with SV. Inhibition of PI3K/Akt caused aberrant remodeling of the actin cytoskeleton, reduced expression of VE-cadherin and claudin-5, and reversed the barrier-protective effects of SV. These findings suggest that SV restores the endothelial barrier via PI3K/Akt activation in HPMECs. Whether SV protects barrier function in an *in vivo* LIRI model will be addressed in future studies.

Conclusions

In conclusion, promotion by SV of lung endothelial barrier repair after OGD/R injury was involved in the inhibition of cytoskeleton remodeling and upregulation of intercellular connections (AJs and TJs), which promoted cell migration and decreased endothelial permeability. These phenomena were mediated by PI3K/Akt signaling in HPMECs. Given its protective effects, SV has potential as a pharmacotherapy for LIRI.

Acknowledgements

The work was supported by Department of Cardiovascular surgery, The central Hospital of Nanyang.

Disclosure of conflict of interest

None.

Address correspondence to: Dr. Wang Zhang, Department of Critical Care Medicine, The First Affiliated Hospital, College of Medicine, Zhejiang University, NO. 79 Qingchun Road, Hangzhou 310003, Zhejiang, PR China. E-mail: ivan91@zju.edu.cn

References

[1] Laubach VE and Sharma AK. Mechanisms of lung ischemia-reperfusion injury. Curr Opin Organ Transplant 2016; 21: 246-252.
[2] Lohser J and Slinger P. Lung injury after one-lung ventilation: a review of the pathophysiologic mechanisms affecting the ventilated and the collapsed lung. Anesth Analg 2015; 121: 302-318.
[3] Huffmyer JL and Groves DS. Pulmonary complications of cardiopulmonary bypass. Best Pract Res Clin Anaesthesiol 2015; 29: 163-175.
[4] Ferrari RS and Andrade CF. Oxidative stress and lung ischemia-reperfusion injury. Oxid Med Cell Longev 2015; 2015: 590987.
[5] Bazzoni G and Dejana E. Endothelial cell-to-cell junctions: molecular organization and role in vascular homeostasis. Physiol Rev 2004; 84: 869-901.
[6] Lusis AJ. Atherosclerosis. Nature 2000; 407: 233-241.
[7] Jackevicius CA, Chou MM, Ross JS, Shah ND and Krumholz HM. Generic atorvastatin and health care costs. N Engl J Med 2012; 366: 201-204.
[8] Mermis JD and Simpson SQ. HMG-CoA reductase inhibitors for prevention and treatment of severe sepsis. Curr Infect Dis Rep 2012; 14: 484-492.
[9] Ma S and Ma CC. Recent developments in the effects of nitric oxide-donating statins on cardiovascular disease through regulation of tetrahydrobiopterin and nitric oxide. Vascul Pharmacol 2014; 63: 63-70.
[10] Bi XY, He X, Zhao M, Yu XJ and Zang WJ. Role of endothelial nitric oxide synthase and vagal activity in the endothelial protection of atorvastatin in ischemia/reperfusion injury. J Cardiovasc Pharmacol 2013; 61: 391-400.
[11] Smeeth L, Douglas I, Hall AJ, Hubbard R and Evans S. Effect of statins on a wide range of health outcomes: a cohort study validated by comparison with randomized trials. Br J Clin Pharmacol 2009; 67: 99-109.
[12] Feng Y. Efficacy of statin therapy in patients with acute respiratory distress syndrome/acute lung injury: a systematic review and meta-analysis. Eur Rev Med Pharmacol Sci 2018; 22: 3190-3198.

[13] Lee MG, Lee CC, Lai CC, Hsu TC, Porta L, Lee M, Chang SS, Chien KL and Chen YM; National Taiwan University Hospital Health Economics and Outcome Research Group. Preadmission statin use improves the outcome of less severe sepsis patients - a population-based propensity score matched cohort study. Br J Anaesth 2017; 119: 645-654.

[14] Fan ZX, Yang CJ, Yang J and Yang J. Stains: anovel therapy thought in myocardial ischemia reperfusion injury other than lipid lowering. Int J Cardiol 2017; 229: 10.

[15] Matsuo S, Saiki Y, Adachi O, Kawamoto S, Fukushige S, Horii A and Saiki Y. Single-dose rosuvastatin ameliorates lung ischemia-reperfusion injury via upregulation of endothelial nitric oxide synthase and inhibition of macrophage infiltration in rats with pulmonary hypertension. J Thorac Cardiovasc Surg 2015; 149: 902-909.

[16] Drolz A, Horvatits T, Michl B, Roedl K, Schellongowski P, Holzinger U, Zauner C, Heinz G, Madl C, Trauner M and Fuhrmann V. Statin therapy is associated with reduced incidence of hypoxic hepatitis in critically ill patients. J Hepatol 2014; 60: 1187-1193.

[17] Craig TR, Duffy MJ, Shyamsundar M, McDowell C, O'Kane CM, Elborn JS and McAuley DF. A randomized clinical trial of hydroxymethylglutaryl-coenzyme a reductase inhibition for acute lung injury (The HARP Study). Am J Respir Crit Care Med 2011; 183: 620-626.

[18] Criner GJ, Connett JE, Aaron SD, Albert RK, Bailey WC, Casaburi R, Cooper JA Jr, Curtis JL, Dransfield MT, Han MK, Make B, Marchetti N, Martinez FJ, Niewoehner DE, Scanlon PD, Sciurba FC, Scharf SM, Sin DD, Voelker H, Washko GR, Woodruff PG and Lazarus SC. Simvastatin for the prevention of exacerbations in moderate-to-severe COPD. N Engl J Med 2014; 370: 2201-2210.

[19] Shyamsundar M, McKeown ST, O'Kane CM, Craig TR, Brown V, Thickett DR, Matthay MA, Taggart CC, Backman JT, Elborn JS and McAuley DF. Simvastatin decreases lipopolysaccharide-induced pulmonary inflammation in healthy volunteers. Am J Respir Crit Care Med 2009; 179: 1107-1114.

[20] He M, Zhang Y, Xie F, Dou X, Han M and Zhang H. Role of PI3K/Akt/NF-kappaB and GSK-3beta pathways in the rat model of cardiopulmonary bypass-related lung injury. Biomed Pharmacother 2018; 106: 747-754.

[21] Liang S, Wang Y and Liu Y. Dexmedetomidine alleviates lung ischemia-reperfusion injury in rats by activating PI3K/Akt pathway. Eur Rev Med Pharmacol Sci 2019; 23: 370-377.

[22] Zhang LJ, Tao BB, Wang MJ, Jin HM and Zhu YC. PI3K p110alpha isoform-dependent Rho GTPase Rac1 activation mediates H2S-promoted endothelial cell migration via actin cytoskeleton reorganization. PLoS One 2012; 7: e44590.

[23] Zhang Y, Li D, Luo J, Chen S, Dou X, Han M and Zhang H. Pharmacological postconditioning with sevoflurane activates PI3K/AKT signaling and attenuates cardiopulmonary bypass-induced lung injury in dog. Life Sci 2017; 173: 68-72.

[24] Zhang D, Li C, Song Y, Zhou J, Li Y, Li J and Bai C. Integrin alphavbeta5 inhibition protects against ischemia-reperfusion-induced lung injury in an autophagy-dependent manner. Am J Physiol Lung Cell Mol Physiol 2017; 313: L384-L394.

[25] Patterson CE, Rhoades RA and Garcia JG. Evans blue dye as a marker of albumin clearance in cultured endothelial monolayer and isolated lung. J Appl Physiol (1985) 1992; 72: 865-873.

[26] Zheng X, Zhang W and Hu X. Different concentrations of lipopolysaccharide regulate barrier function through the PI3K/Akt signalling pathway in human pulmonary microvascular endothelial cells. Sci Rep 2018; 8: 9963.

[27] Zhang W, Zhang Y, He Y, Wang X and Fang Q. Lipopolysaccharide mediates time-dependent macrophage M1/M2 polarization through the Tim-3/Galectin-9 signalling pathway. Exp Cell Res 2019; 376: 124-132.

[28] Silva PL, Pelosi P and Rocco PRM. Personalized pharmacological therapy for ARDS: a light at the end of the tunnel. Expert Opin Investig Drugs 2020; 29: 49-61.

[29] Christophe B, Karatela M, Sanchez J, Pucci J and Connolly ES. Statin therapy in ischemic stroke models: aMeta-analysis. Transl Stroke Res 2020; 11: 590-600.

[30] Yu Y, Jing L, Zhang X and Gao C. Simvastatin attenuates acute lung injury via regulating CDC42-PAK4 and endothelial microparticles. Shock 2017; 47: 378-384.

[31] Mouneimne G, Hansen SD, Selfors LM, Petrak L, Hickey MM, Gallegos LL, Simpson KJ, Lim J, Gertler FB, Hartwig JH, Mullins RD and Brugge JS. Differential remodeling of actin cytoskeleton architecture by profilin isoforms leads to distinct effects on cell migration and invasion. Cancer Cell 2012; 22: 615-630.

[32] Mehta D and Malik AB. Signaling mechanisms regulating endothelial permeability. Physiol Rev 2006; 86: 279-367.

[33] Zhang Y, Zhang L, Li Y, Sun S and Tan H. Different contributions of clathrin- and caveolae-mediated endocytosis of vascular endothelial cadherin to lipopolysaccharide-induced vascular hyperpermeability. PLoS One 2014; 9: e106328.

[34] Huang LY, Stuart C, Takeda K, D'Agnillo F and Golding B. Poly(I:C) induces human lung endothelial barrier dysfunction by disrupting tight junction expression of claudin-5. PLoS One 2016; 11: e0160875.

[35] Laakkonen JP, Lappalainen JP, Theelen TL, Toivanen PI, Nieminen T, Jauhiainen S, Kaikkonen MU, Sluimer JC and Yla-Herttuala S. Differential regulation of angiogenic cellular processes and claudin-5 by histamine and VEGF via PI3K-signaling, transcription factor SNAI2 and interleukin-8. Angiogenesis 2017; 20: 109-124.

[36] Akizuki R, Shimobaba S, Matsunaga T, Endo S and Ikari A. Claudin-5, -7, and -18 suppress proliferation mediated by inhibition of phosphorylation of Akt in human lung squamous cell carcinoma. Biochim Biophys Acta Mol Cell Res 2017; 1864: 293-302.

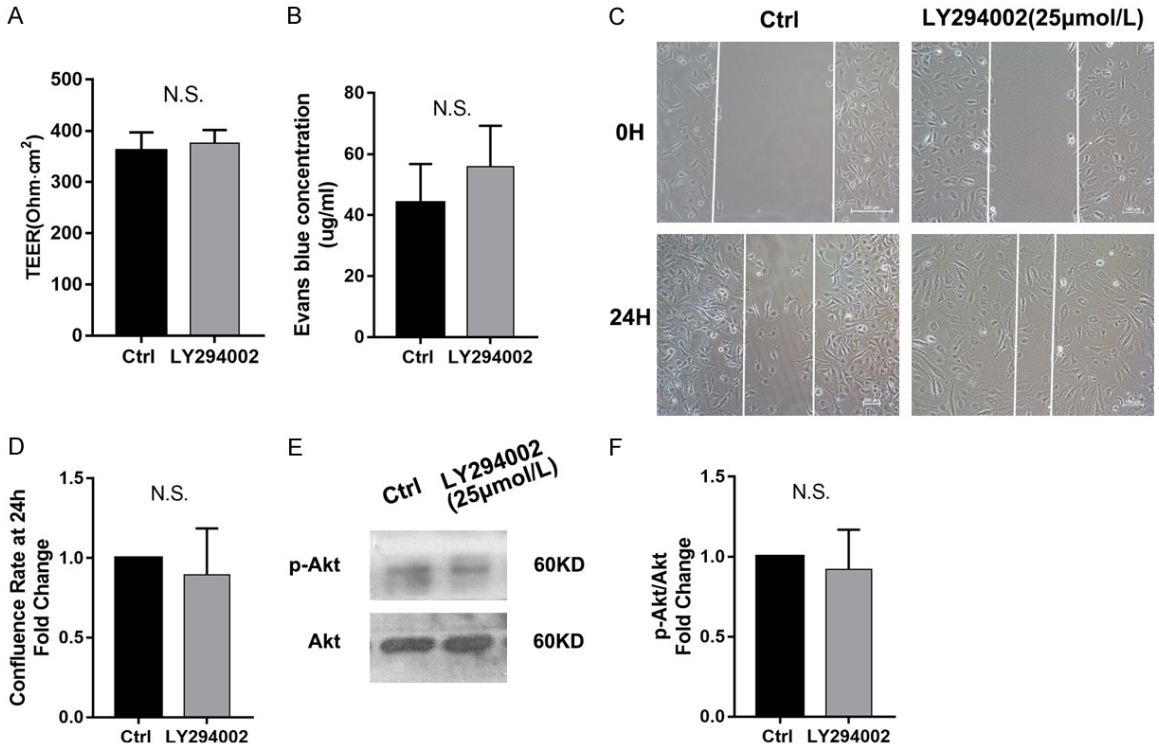

Figure S1. Changes of TEER, monolayer permeability, migration and Akt phosphorylation in HPMECs treated with LY294002 (25 μmol/L). (A-E) The LY294002 has no significant effect on TEER (A), monolayer permeability (B), cell migration (C, D) and Akt phosphorylation (E, F) of untreated HPMECs. scale bars: 200 μm.